Micro-/Nanofluidics

DOI: 10.1002/anie.200604502

NMR Study of Water Molecules Confined in Extended Nanospaces**

*Takehiko Tsukahara, Akihide Hibara, Yasuhisa Ikeda, and Takehiko Kitamori**

The study of water in confined geometries has been receiving much attention in chemistry, biology, and geology.[1] A variety of spectroscopic and theoretical investigations have demonstrated that water molecules confined in 1-nm-scale materials such as porous silica show unique properties not seen on the bulk scale.[2–7] A 1-nm-scale space is available as an experimental space for characterizing the behavior of an individual single molecule, while this scale is too small to illuminate the collective behaviors of liquid-phase molecules as condensed-phase matter. To elucidate the complicated properties of liquid-phase water molecules, a 10–100-nm-scale space is appropriate but has been almost unavailable. The technologies involved in micro- and nanochemistry on a chip are expected to allow the production of a physicochemically well-defined 10–10-nm-scale space on glass substrates (called an extended nanospace). Previously, we developed extended nanospaces by means of well-controlled micro-/nanofabrication techniques and made capillary and time-resolved fluorescence measurements of water confined in the spaces.[8] The results showed that, compared with bulk water, the water confined in the extended nanospaces had a higher viscosity and a lower dielectric constant. Similar size-confinement phenomena have been shown in hydrodynamic flow, conductivity, and ionic transport results in extended nanospaces.[9–12] However, little molecular-level information is available concerning the mechanisms for the novel confinement-induced nanospatial properties of water molecules in extended nanospaces. Here we present size-confinement effects of the molecular structure, motions, protonic mobility, and localization of proton-charge distribution of water and water–surface proton exchange in 295–5000-nm extended nanospaces by NMR spectroscopy measurements.

First, we examined the ^{1}H NMR chemical shift (δ_H) of water in spaces of 295 to 5000 nm at 25 °C and found that the values for the confined water are almost constant at around $\delta_H = 4.6$ ppm, regardless of the sizes (see Supporting Information). This result indicates that the water molecules confined in extended nanospaces keep the four-coordinated hydrogen-bond structures seen for bulk water. However, the full line width at half-height in the ^{1}H NMR spectrum broadened with a decrease in the size of the space (R). Thus, we examined the size dependence of the spin-lattice relaxation rate (^{1}H $1/T_1$) for water at 25 °C. As shown in Figure 1 A, the $1/T_1$ values for confined water molecules increase sharply below $R = 800$ nm whereas they remain almost constant for space sizes of 800–5000 nm. The $1/T_1$ value of 1.62 s^{-1} for a 320-nm space exceeds, by about a factor of 5, the bulk value (0.32 s^{-1}) and is not consistent with $1/T_1$ values for physisorbed water.[13,14] A frequency dependence could also be observed in these ^{1}H $1/T_1$ values (see Supporting Information). These phenomena lead to the interesting conclusion that the molecular motions of water even in extended nanospaces are inhibited compared to those of bulk water.

However, the interpretation of the measured ^{1}H $1/T_1$ ($1/T_{1\,meas}$) values, which involve both an intramolecular component ($1/T_{1\,intra}$) associated with rotational diffusion and an intermolecular one ($1/T_{1\,inter}$) associated with translational diffusion and proton diffusion, is difficult. It is desirable to extract the $1/T_{1\,intra}$ component by measuring the ^{2}H $1/T_1$ value of heavy water (D_2O), which has a quadrupole moment, because the obtained ^{2}H $1/T_1$ values are dependent on rotational correlation times (τ_C) for the motion of the deuterium electric-field gradient (EFG) tensor.[15,16] The value of τ_C for H_2O is about 1.4-times larger than that of D_2O because of the isotope effect on the viscosity of water, and so the $1/T_{1\,intra}$ component of H_2O can be determined.[17] With the relation $1/T_{1\,meas} = 1/T_{1\,intra} + 1/T_{1\,inter}$, it becomes possible to divide the size dependence of $1/T_{1\,inter}$ and $1/T_{1\,intra}$ for H_2O (see Supporting Information). As shown in the inset in Figure 1 A, $1/T_{1\,intra}$ is almost constant for all sizes, with the main effect of size being on the $1/T_{1\,inter}$ component, yet without any change in structure. It follows from this result that the motional properties of water confined in extended nanospaces are quite different from those in 1-nm-scale nanomaterials, because in such nanomaterials not only translation but also rotation is inhibited for water molecules.[3]

The variation in only intermolecular interaction results from inhibition of molecular translational diffusion and/or enhancement of proton diffusion associated with the Grotthus proton-transfer mechanism:[18] $H_3O^+ + H_2O \rightarrow H_2O + H_3O^+$. Therefore, we measured the temperature dependence of the ^{1}H $1/T_1$ values over the range of 4 to 50 °C and examined the size dependence of the apparent activation energy (E_a) values taken from the Arrhenius plots for ^{1}H $1/T_1$. If molecular translational diffusion is dominantly affected by size confinement, the E_a values should increase because of an increase in the potential-energy barrier to translation. How-

[*] Dr. T. Tsukahara, Dr. A. Hibara, Prof. T. Kitamori
Department of Applied Chemistry
School of Engineering
The University of Tokyo
7-3-1 Hongo, Bunkyo, Tokyo 113-8656 (Japan)
Fax: (+81) 3-5841-6039
E-mail: kitamori@icl.t.u-tokyo.ac.jp
Prof. Y. Ikeda
Research Laboratory for Nuclear Reactors
Tokyo Institute of Technology
2-12-1 O-Okayama, Meguro, Tokyo 152-8550 (Japan)

[**] This work was financially supported by the Core Research for Evolutional Science and Technology (CREST), Japan Science and Technology Corporation (JST).

Supporting information for this article is available on the WWW under http://www.angewandte.org or from the author.

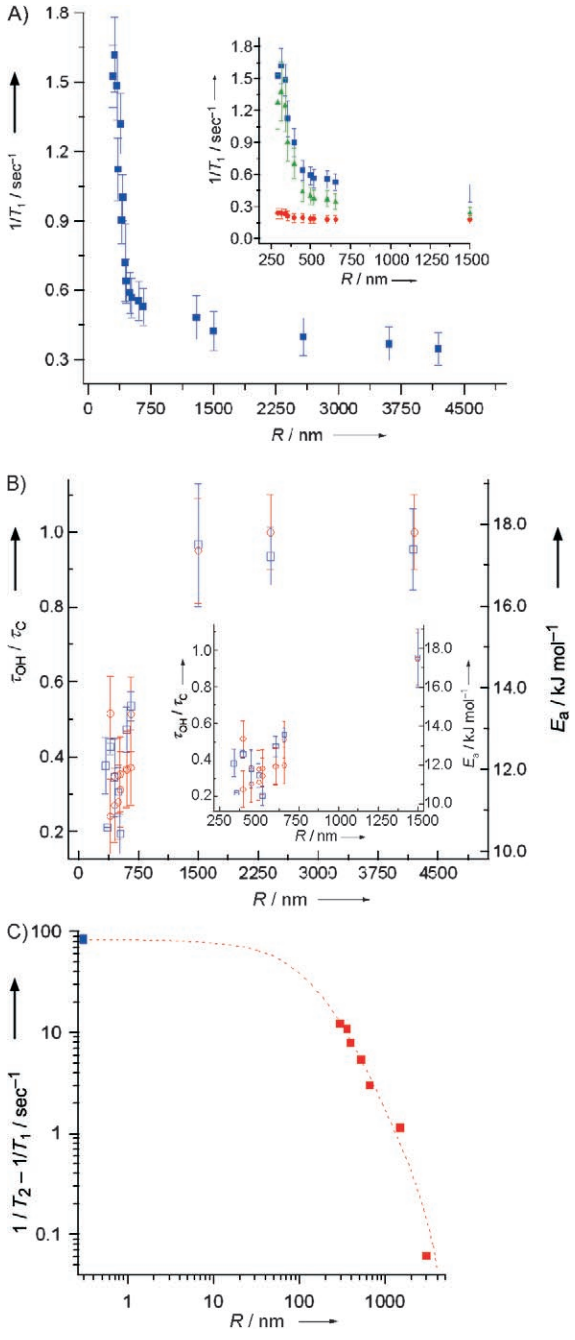

Figure 1. A) The size dependence of ^{1}H $1/T_1$ values (■) of water confined in micro- and nanospaces at 300 MHz and 22 °C. The inset shows the size dependence of intermolecular translational (▲) and intramolecular rotational motions (●) obtained from experimental ^{1}H $1/T_1$ (■) values of water in the channel range of 295 to 1500 nm. The ^{1}H $1/T_1$ values were measured by the inversion recovery method ($\pi-\tau-\pi/2{\cdot}5\,T_1$) with τ varying from 1 ms to 20 s and expressed by a single-exponential function. B) The size dependences of τ_{OH}/τ_C ratios (○) and E_a values (□) for water inside micro- and nanospaces at 300 MHz and 22 °C. The inset shows the results for 295–1500-nm spaces. C) A log–log plot of $1/T_2-1/T_1$ values (■) versus space sizes of water at 300 MHz and 22 °C. The $1/T_2-1/T_1$ values increase continuously from bulk water to adsorbed water (■; see Refs. [13, 14]). The ^{1}H $1/T_2$ measurements were performed using a standard Carr–Purcell–Meiboom–Gill (CPMG) pulse sequence ($\pi/2-\tau-\pi-2\tau-\pi-2\tau-\pi\cdots$) with 2τ pulse spacing of 0.987 ms.

ever, as shown in Figure 1 B (blue squares), the E_a value of bulk water is 18 kJ mol^{-1} and the value decreases to 10 kJ mol^{-1} with a decrease in size to $R = 320$ nm. This loss of 8 kJ mol^{-1} means that the size confinement has reduced the potential-energy barrier to the proton diffusion of water. In other words, rather than hydrodynamic mobility it is protonic mobility, including proton hopping between water molecules, that dominates the molecular behavior in confining geometries. This explanation is supported by the fact that the 8 kJ mol^{-1} decrease in energy shown above corresponds to the differences in E_a values between dielectric relaxation and proton-hopping times.[17,19]

When the proton-transfer mechanism is modulated, the proton-charge distributions should be localized along linear O···HO hydrogen-bonding chains of water molecules. The ratio of the τ_C value to the rotational correlation times obtained from the ^{1}H $1/T_1$ values in ^{17}O-enriched water (τ_{OH}) can provide a criterion for evaluating the localization of proton-charge distribution, because the principal axis of the deuterium EFG tensor is essentially coincident with an O–H internuclear vector.[16] In a normal liquid, the ^{17}O-induced ^{1}H $1/T_1$ values depend only on rotational motions as in the case of D_2O and the τ_{OH} values should approximately equal the τ_C values. When the proton-charge distribution along the O···HO hydrogen-bonding chain is localized by the appearance of intermolecular interactions between a proton and ^{17}O, the τ_{OH}/τ_C ratios should be less than unity (see Supporting Information). The plot of R versus τ_{OH}/τ_C in Figure 1 B (red circles) is a curve of similar shape to that of E_a and shows that the ratio decreases significantly from unity to about 0.3 in the same size range as for the ^{1}H $1/T_1$ values.

Although the ^{1}H $1/T_1$ values provide insight into the faster component of motions, it is insensitive to the slower ones. The slower motions are usually found in the water molecules adsorbed on surfaces where the water molecules form ordered water layers invoking a linear O···H–O bond near the surface.[20,21] Therefore, to estimate the correlation between water adsorbed on surfaces and water in extended nanospaces, we measured the ^{1}H spin–spin relaxation rates (^{1}H $1/T_2$) governed by the slower component of molecular motions.[15,22] We found that size confinement increases the $1/T_2$ values just as it did for the $1/T_1$ values, while the differences between the $1/T_2$ and $1/T_1$ values become greater with reductions in the nanospace sizes as shown in Figure 1 C. Since the chemical exchange of magnetization between protons in water and surfaces should be reflected in these differences, their increase by size confinement corresponds to an enhancement of the frequency of proton exchanges between water molecules.

The important findings in the NMR results of the confined water are as follows: 1) retention of the four-coordinated water structure, 2) slower translational motions, 3) dominant protonic mobility, 4) proton-charge distribution localized along the O···H-O hydrogen-bonding chains, and 5) chemical exchange of protons between water and water adsorbed on surfaces (Figure 2 A). These results indicated that protons migrate through water–water and/or water–surface hydrogen-bonding networks. We can hypothesize that, as illustrated in Figure 2 B, the water molecules in extended nanospaces

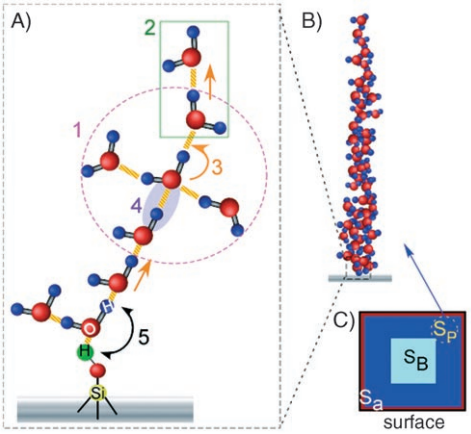

Figure 2. A) Schematic illustration of water molecules confined in extended nanospaces on a glass chip. 1) The O–O distance between water molecules and the bulk water structure are retained in the extended nanospaces. 2) The intermolecular translational motions in extended nanospaces are affected by size confinement. 3) Protons migrate from one water molecule to another adjacent one through hydrogen-bonding networks. 4) Proton-charge distribution is localized along its linear O···H-O hydrogen-bonding chains. 5) Chemical exchange of protons between water and silanol groups on the surfaces enhances protonic mobility of water in extended nanospaces. B) Schematic illustration of loosely coupled water molecules located within 10–100 nm of a glass/water interface. C) Schematic illustration of the three phases composed in extended nanospaces on a glass chip. In the illustration of a nanospace, the light blue (S_B), dark blue (S_P), and red (S_a) phases correspond to the regions associated with the bulk phase, a proton-transfer phase, and an adsorbed water phase, respectively.

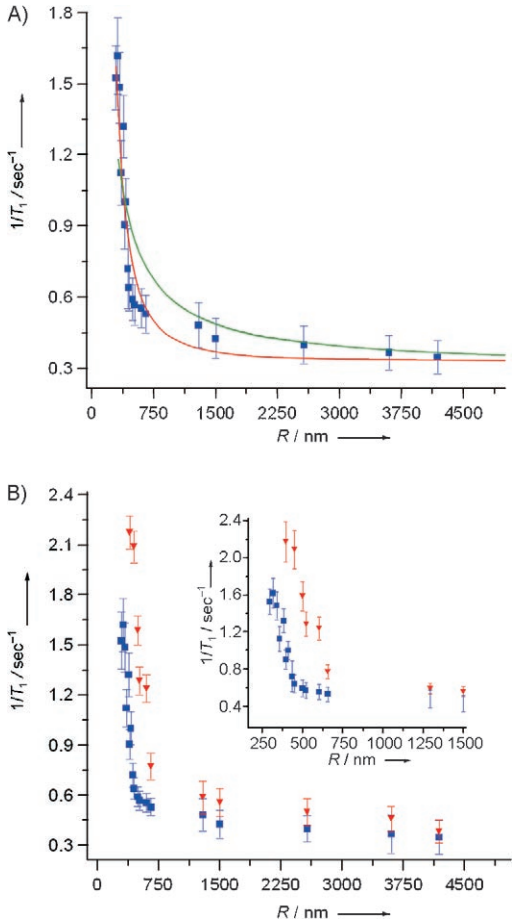

Figure 3. A) Comparison of the size dependence of experimental $1/T_1$ values (■) and theoretical $1/T_1$ values. The solid red and green lines represent fits of the $1/T_1$ values based on a three-phase exchange theory [Eq. (1)] and a two-phase exchange theory, respectively. B) The size dependence of ^{1}H -$1/T_1$ values in an unmodified case (■) and a modified case (▼) for water confined in micro- and extended nanospaces at 300 MHz and 22 °C. The inset shows an expanded view over the 250–1500 nm range. The glass surface was modified with trimethylchlorosilane to introduce hydrophobic $Si(CH_3)_3$ groups, which interact less with water.

loosely couple in a direction perpendicular to the surface. Specifically, we suggest that a proton-transfer phase (S_P), which is an intermediate phase between a bulk phase (S_B) and the adsorbed phase (S_a), exists in extended nanospaces as shown in Figure 2C.

To verify the validity of this model, we compared our experimental relaxation data with a theoretical one based on three-phase exchange theory, which states that the water in confined geometries is composed of three phases: S_B, S_P, and S_a. The water molecules in spaces within the 800–5000-nm-size range are dominated by the S_B phase, and their relaxation rates do not depend on the size of the space. As the S_P phase appears with decreasing sizes at around 800 nm, the relaxation rates begin to change according to the interfacial area ratio of S_P to S_B. For all confinement sizes, the S_a phase exists in a thickness of about 0.3 nm.[14] Thus, the overall relaxation rate ($1/T_{1\,exptl}$) is expressed as follows [Eq. (1)] as the weighted

$$\frac{1}{T_{1\,exptl}} = \frac{1}{T_{1B}} + \frac{\lambda A_1}{V_1}\frac{1}{T_{1P}} + \frac{\varepsilon A_2}{V_2}\frac{1}{T_{1a}} \qquad (1)$$

average of these phases; the subscripts 1 and 2 denote S_P and S_a phases, respectively, λ refers to the thickness of S_a, ε corresponds to the thickness of thickness of S_P, and A/V represents the interfacial area ratio.

When the thickness (ε) of S_P was presumed to be 50 nm, the values calculated by Equation (1) were quite consistent with the measured $1/T_1$ data (Figure 3A; red line). On the other hand, the relaxation rates given by a well-known two-phase exchange theory, which takes into account only the exchange of water between the S_B and the S_a phases,[20,23] diverged from the experimentally measured ^{1}H $1/T_1$ values (Figure 3A; green line). Evidently, the S_P phase plays an important role in determining water behaviors in extended nanospaces.

To assess the relative contribution of the water–surface interface, the well-established technique of surface modification provides a very useful approach. Thus, we compared the size dependence of the ^{1}H $1/T_1$ values for water confined by an unmodified hydrophilic surface including OH groups and those by a modified hydrophobic surface including CH_3 groups. The results are shown in Figure 3B, and the $1/T_1$ values of water confined in the modified surface were found to increase at around $R = 1000$ nm. Despite the fact that the interactions of the water molecules with the CH_3 groups were

weaker than those with the OH groups, the size-confinement effect in the hydrophobic case appeared stronger than that in the hydrophilic case. The differences between the hydrophilic and hydrophobic cases ($\approx$ 200 nm) are probably generated by hydrophobic hydration surrounding the CH_3 groups, because hydrophobic surfaces immersed in water generate a long-range attractive force with a range of 100 nm.[24–26] Apparently, therefore, the highly directional hydrogen-bonding networks accompanied by hydrophobic hydration promote the formation of coupled water molecules as illustrated in Figure 2.

In summary, we have employed NMR spectroscopy results to characterize the molecular structure and dynamics of water confined in extended nanospaces and have confirmed that a S_P phase, which consists of loosely coupled water molecules located within about 50 nm from a glass/water interface, exists in extended nanospaces. Our NMR results will have important implications for both understanding the behavior of nanofluidics and the molecular physical chemistry of liquid-phase molecules and implementing micro- to nanofluidic devices.

Experimental Section

The extended nanospaces were fabricated on high-purity synthetic quartz glass substrates with impurities at less than 1 ppb (VIOSIL-SX, ShinEtsu Quartz Co., Ltd.) by electron-beam lithography and plasma etching. All fabricated spaces had widths (W) of 360–5000 nm, depths (D) of 250–5000 nm, and a length of 42 mm. As the cylindrical pores with diameter (R) were replaced by $4/R$ on the basis of the surface-to-volume ratio ($2(D+W)/DW$), all results could be optimized as an equivalent diameter R (295–5000 nm). The substrate fabricated with extended nanospaces was thermally laminated with a cover plate in a vacuum furnace at 1080 °C and then cut with a diamond cutter to a size that allowed it to be inserted into a commercial 5-mm NMR sample tube. All ultrapure water samples were treated with a water purification system composed of reverse osmosis membrane, ion-exchange cylinder, and UV sterilizer (MINIPURE TW-300RU, Nomura Micro Science Co., Ltd.), and had specific resistivity greater than 18.0 MΩ cm. Highly purified water was degassed through a number of freeze–pump–thaw cycles and was then introduced into the extended nanospaces by means of capillary force under an argon atmosphere. The ^{17}O-enriched water sample (ISOTEC Inc.; 4% and 8%) was used without purification. The water-filled spaces were sealed, and the substrate was put into an NMR sample tube. All NMR spectra of water were measured at 4–50 °C without spinning. The effects of dust and impurities could be excluded by performing all operations in class-100 and -1000 clean rooms.

Received: November 3, 2006

Keywords: confinement effects · molecular dynamics · nanotechnology · NMR spectroscopy

[1] V. Buch, J. P. Devlin, *Water in Confining Geometries* Springer, Berlin, **2003**.
[2] K. Koga, G. T. Gao, H. Tanaka, X. C. Zeng, *Nature* **2001**, *412*, 802–805.
[3] R. A. Farrer, J. T. Fourkas, *Acc. Chem. Res.* **2003**, *36*, 605–612.
[4] F. Bruni, M. A. Ricci, A. K. Soper, *J. Chem. Phys.* **1998**, *109*, 1478–1485.
[5] J. N. Israelachvili, H. Wennerström, *Nature* **1996**, *379*, 219–225.
[6] R. Bergman, J. Swenson, *Nature* **2000**, *403*, 283–286.
[7] B. Grünberg, T. Emmler, E. Gedat, L. Shenderovich, G. H. Findenegg, H.-H. Limbach, G. Buntkoesky, *Chem. Eur. J.* **2004**, *10*, 5689–5696.
[8] A. Hibara, T. Saito, H. B. Kim, M. Tokeshi, T. Ooi, M. Nakao, T. Kitamori, *Anal. Chem.* **2002**, *74*, 6170–6176.
[9] N. R. Tas, P. Mela, T. Kramer, J. W. Berenschot, A. van den Berg, *Nano Lett.* **2003**, *3*, 1537–1540.
[10] S. Liu, Q. Pu, Li. Gao, C. Korzeniewski, C. Matzke, *Nano Lett.* **2005**, *5*, 1389–1393.
[11] Q. Pu, J. Yun, H. Temkin, S. Liu, *Nano Lett.* **2004**, *4*, 1099–1103.
[12] N. Kaji, R. Oguma, A. Oki, Y. Horiike, M. Tokeshi, Y. Baba, *Anal. Bioanal. Chem.* **2006**, 386, 759–764.
[13] K. Overloop, L. Van Gerven, *J. Magn. Reson. Ser. A* **1993**, *101*, 147–156.
[14] F. D'Orazio, J. C. Tarczon, W. P. Halperin, K. Eguchi, T. Mizusaki, *J. Appl. Phys.* **1989**, *65*, 742–751.
[15] T. C. Farrar, E. D. Becker, *Pulse and Fourier Transform NMR*, Academic Press, New York, **1971**.
[16] R. Ludwig, F. Weinhold, T. C. Farrar, *J. Chem. Phys.* **1995**, *103*, 6941–6950.
[17] N. Agmon, *J. Phys. Chem.* **1996**, *100*, 1072–1080. Errata: N. Agmon, *J. Phys. Chem.* **1997**, *101*, 4352.
[18] A. A. Kornyshev, A. M. Kuznetsov, E. Spohr, J. Ulstrup, *J. Phys. Chem. B* **2003**, *107*, 3351–3366.
[19] B. Cohen, D. Huppert, *J. Phys. Chem. A* **2003**, *107*, 3598–3605.
[20] S. G. Allen, P. C. L. Stephenson, J. H. Strange, *J. Chem. Phys.* **1997**, *106*, 7802–7809.
[21] J. H. Strange, J. Mitchell, J. B. W. Webber, *Magn. Reson. Imaging* **2003**, *21*, 221–226.
[22] S. Meibom, *J. Chem. Phys.* **1961**, *34*, 375–388.
[23] K. R. Brownstein, C. E. Tarr, *J. Magn. Reson.* **1977**, 26, 17–24.
[24] G. Gompper, M. Hauser, A. A. Kornyshev, *J. Chem. Phys.* **1994**, *101*, 3378–3389.
[25] P. Attard, *Adv. Colloid Interface Sci.* **2003**, 104, 75–91.
[26] S. Singh, J. Houston, F. van Swol, C. J. Brinker, *Nature* **2006**, *442*, 526.

